PERFORMANCE AND DESIGN OF PRECISION-CAST SHAPE MEMORY ALLOY BRAIN SPATULA

HISAAKI TOBUSHI, KENTO MITSUI, KOHEI TAKEDA

Aichi Institute of Technology, Department of Mechanical Engineering, Toyota, Japan

e-mail: tobushi@aitech.ac.jp

KAZUHIRO KITAMURA

Aichi University of Education, Department of Technology Education, Kariya, Japan

YUKIHARU YOSHIMI

Yoshimi Inc., Obu, Japan

In order to develop a brain spatula made of a shape memory alloy (SMA), this paper discusses the bending characteristics of a new brain spatula precision-cast in a TiNi SMA. The results obtained can be summed up as follows. (1) With respect to an SMA-brain spatula having the same length and width as the existing type made of copper, if the new cast SMA spatula is 1.2 times as great in thickness as the existing copper spatula, or if a conventionally rolled SMA spatula is 1.3 times as great, the SMA instrument will offer the same bending rigidity and withstand almost as great a bending force as the copper one. (2) Expressing the bending fatigue life of the copper or SMA in the region of low-cycle fatigue as a power function of the maximum bending strain, the fatigue life of the SMA is longer than that of the copper. For both the cast and the rolled SMAs, the fatigue life is longer under pulsating-plane bending than under alternating plane bending.

Key words: shape memory alloy, brain spatula, bending

1. Introduction

The shape memory effect (SME) and superelasticity (SE) are characteristic behaviors of a shape memory alloy (SMA). A strain of several percent can be recovered by heating in the case of the SME or unloading in the case of SE. These behaviors occur due to the martensitic transformation (MT) and its reverse transformation. The large recovery stress and great amounts of energy dissipation and storage associated with the MT are effectively exploited in an SMA (Funakubo, 1987; Duerig *et al.*, 1990; Saburi, 2000; Chu and Zhao, 2002; Otsuka and Wayman, 1998). The development of applications for SMAs as intelligent materials has therefore attracted worldwide attention. SMAs are now in use across wide fields of industry, electrical manufacturing, and medical and leisure technologies, to name only a few.

A brain spatula or brain retractor is an instrument used in surgery to hold a brain incision open while a deep cerebral tumor is operated on. A schematic image of how this is done is shown in Fig. 1. As shown, the spatula is used in a bent form, fitting the shape and depth of the individual brain. After the operation, the spatula is struck with a miniature hammer to return it to its original flat form, after which it is sterilized by heating and is then ready for reuse. The usual material for brain spatulas hitherto has been copper, but owing to the irrecoverable loss of evenness that develops on the copper surface after each use, in practice the instrument has to be disposed of after being used only a few times. If an SMA material is used instead, the original flat shape can be restored automatically and precisely through the working of the SME during the sterilization heating in the autoclave. This not only saves time and dispenses with

the need for hammering, but also means that the unevenness left from plastic deformation is much reduced so that the spatula can be reused over and over.
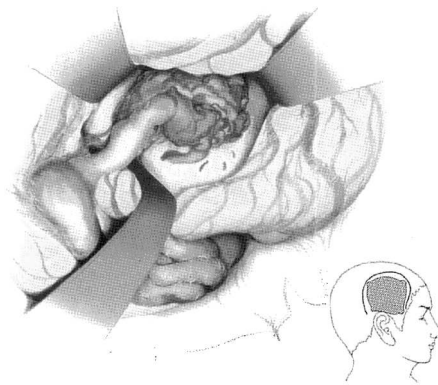

Fig. 1. Illustration of a brain spatula in surgical use

The instruments treated in this study have been recently developed and are precision-cast in a lost-wax process of the self-combustion high-temperature synthesis method (Yoshimi *et al.*, 2008). The brain spatula needs to form itself into unique shapes according to the brain configurations of individual patients and, as can be seen from the examples in Fig. 2, the spatulas themselves also come in intricate forms that are a challenge to create in the TiNi SMA material. The precision casting technique makes it much easier for these tools to be manufactured.
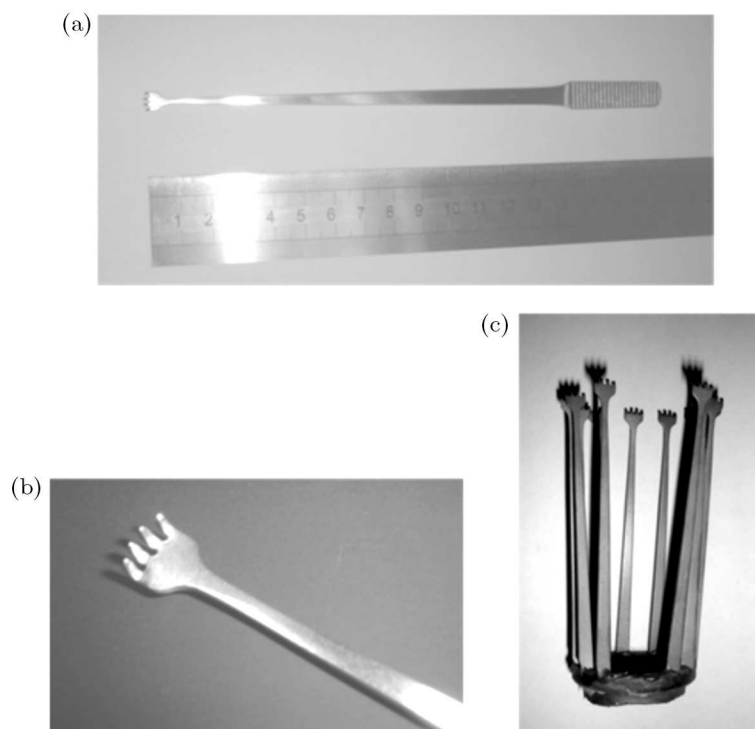
(a)

(c)

(b)

Fig. 2. Examples of precision-cast TiNi SMA brain spatulas; (a) whole rake-type brain spatula against a centimeter scale, (b) tip of the rake-type brain spatula, (c) batch of brain spatulas just after precision casting

The conditions required of a brain spatula are, first, that it can be bent to any desired shape to fit the brain being operated on and, second, that it should have sufficient rigidity to be able to keep the brain incision open during the operation. These requirements can be specified in terms of the bending deformation properties of the instrument, including its bending rigidity. To

evaluate the reliability of a brain spatula from the point of view of safety, the fatigue properties of the material are crucial, and to investigate these, the spatula has to be subjected to cyclic plane bending. This paper is the first reported study of the plane bending properties of a TiNi SMA considered as the material for a brain spatula.

For the present study, in pursuit of the development of the SMA brain spatula, tension tests were conducted to examine stress-strain relations in three materials: the newly introduced cast TiNi SMA, a TiNi SMA of the conventional rolled type, and copper of the type used in brain spatulas up until now. The shape and dimension requirements of an SMA brain spatula were investigated on the basis of the bending deformation properties of a strip cantilever. Further, an investigation was also conducted into the fatigue properties of the materials, which is a question of extreme importance for the practicalities of their cyclic use.

2. Experimental method

2.1. Materials and specimens

The materials used in the experiment were a new-type cast Ti-49.7at%Ni SMA, a conventional rolled Ti-50.0at%Ni SMA, and copper as used in brain spatulas hitherto. The new cast SMA was produced by precision casting using a lost-wax process from a self-combustion high-temperature synthesis method (Yoshimi *et al.*, 2008). Samples of the cast and rolled SMAs were shape-memorized by fixing them in a flat plane for 40 min at a furnace temperature of 753 K and then quenching them in water. The starting and finishing temperatures for the MT of the SMAs, M_s and M_f, and those for the reverse transformation, A_s and A_f, were obtained from the DSC (differential scanning calorimetric) tests. The values obtained were $M_s = 326$ K, $M_f = 312$ K, $A_s = 342$ K, $A_f = 365$ K for the rolled SMA and $M_s = 358$ K, $M_f = 283$ K, $A_s = 314$ K, $A_f = 386$ K for the cast SMA. The specimens used in the tension tests were the uniform rectangular bars with a thickness $t = 1.0$ mm, width $w = 1.2$ mm and length $l = 160$ mm for the rolled and cast SMAs, with corresponding values of $t = 1.0$ mm, $w = 8.5$ mm and $l = 140$ mm for the copper. In the fatigue tests, all specimens were bars with dimensions of $t = 1.0$ mm, $w = 1.2$ mm and $l = 80$ mm.

2.2. Experimental apparatus

An SMA characteristic-testing machine was used for the tension test (Tobushi *et al.*, 1992). The testing machine was composed of a tension control for loading and unloading and a heating-cooling device to control temperature. Displacements of the specimen were measured using an extensometer with a gauge length of 50 mm.
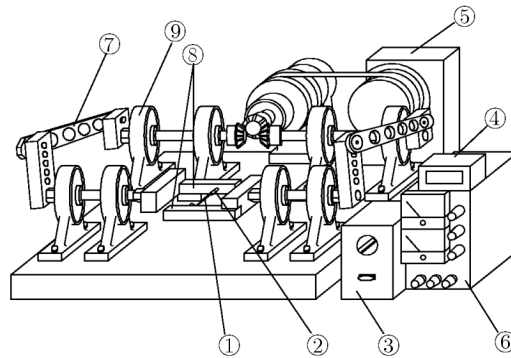

Fig. 3. Experimental apparatus for alternating-plane bending fatigue test; ① specimen, ② grip, ③ speed controller, ④ cycle counter, ⑤ motor, ⑥ power source, ⑦ crank 1, ⑧ crank 2, ⑨ bearing

A machine for the testing of alternating-plane bending fatigue (Furuichi *et al.*, 2003), for use in the fatigue tests, is shown in Fig. 3. In the fatigue testing, the maximum bending strain occurs in the central part of the specimen ①, and the tensile and compressive bending strains occur alternately. Use was also made in the fatigue tests of a machine for the testing of pulsating-plane bending fatigue (Tobushi *et al.*, 2001). In the alternating- and pulsating-plane bending tests, the maximum bending strain on the surface of the specimen was selected and the number of cycles to failure was obtained under a constant frequency. A scanning electron microscope (SEM) was used to observe the fracture surface of the specimen.

2.3. Experimental procedure

The tension tests were carried out under a constant strain rate in air at room temperature below the M_f point of the SMA bars. Since the yielding of the SMA occurs under low stress in the M-phase, the SMA-brain spatula can be bent with a very small force. In the case of SMA bars in the M-phase, a residual strain appears after unloading. SMA bars showing the residual strain were heated up to temperatures above the A_f point under no load. In this heating process of the SMA bars, the residual strain was found to diminish due to the reverse transformation between the A_s and A_f points.

The tests for alternating- and pulsating-plane bending fatigue were carried out in air at room temperature. Every specimen fractured in the central part of its length between the grips, which is where the bending strain reaches its maximum value. The maximum bending strain ε_m on the surface of the specimen was obtained from the radius of curvature at the point of fracture. The frequency f was found to be 8.33 Hz (500 cpm) and 3.33 Hz (200 cpm), respectively.

3. Deformation properties of materials used for brain spatula

3.1. Tensile deformation properties

The stress-strain curves of the copper, the rolled and the cast SMAs obtained from the tension test under a strain rate of $d\varepsilon/dt = 2 \cdot 10^{-4}\,\mathrm{s}^{-1}$ are shown in Fig. 4. As can be seen in Fig. 4, a linear elastic deformation occurs in the initial loading stage and yielding occurs thereafter. The modulus of elasticity E determined from the slope of the initial stress-strain
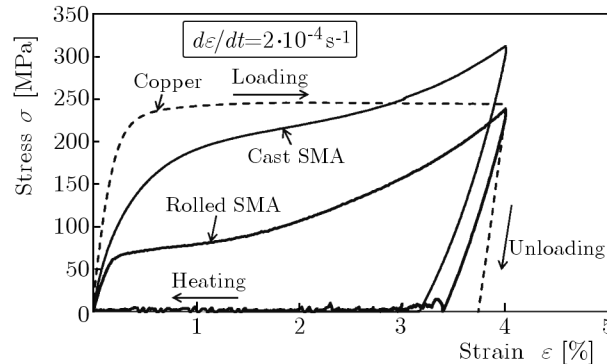

Fig. 4. Tensile stress-strain curves for copper, rolled SMA and cast SMA as materials for brain spatulas

curve is 40 GPa for the rolled SMA, 54 GPa for the cast SMA and 95 GPa for the copper. Approximating the elastic and yield regions of the stress-strain curves to two straight lines, the yield stress σ_M was determined from the intersection of these lines. This gave a value of 68 MPa for the rolled SMA, 168 MPa for the cast SMA and 240 MPa for the copper. In the case of the copper, the deformation seen at strain levels of above 0.2% occurs due to plastic

deformation with dislocations. For example, in the unloading process from a strain of 4%, there is a strain recovery of 0.25% corresponding to the elastic deformation, leaving the residual strain as permanent strain. In the cases of the SMAs, however, since the material is in the M-phase at room temperature below the M_f point, yielding occurs due to rearrangements in the M-phase. In the unloading process from the same strain of 4%, there is a strain recovery of 0.6% for the rolled, and 0.8% for the cast SMA, leaving the residual strains of 3.4% and 3.2% respectively after unloading.
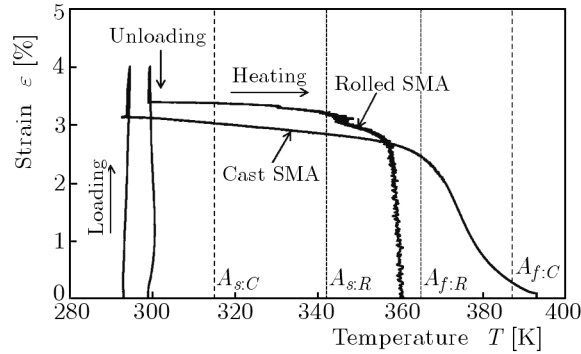

Fig. 5. Strain-temperature curves for the rolled and cast SMA in tension, with unloading followed by heating without loading

The relationships between strain and temperature for the cast and rolled SMAs, obtained from tension tests with unloading followed by heating in the absence of load, are shown in Fig. 5. The symbols $A_{s:C}$, $A_{s:R}$, $A_{f:C}$ and $A_{f:R}$ in Fig. 5 represent the starting and finishing temperatures for the reverse-transformation in the cases of the cast and rolled SMAs, respectively. In the heating process under no load, strain begins to recover gradually around A_s and disappears altogether around A_f. The SME behind this strain recovery occurs as a result of the reverse transformation from the M-phase to the parent (austenite) phase.

3.2. Comparison of characteristic values for deformation

Table 1 sets out the values of the modulus of elasticity E, the yield stress σ_M, the yield strain ε_M and the hardening modulus k for the copper, the rolled and the cast SMAs materials, as obtained from the tension tests. As can be seen, both the modulus of elasticity and the yield stress are lower for the rolled and the cast SMAs than for the copper. These differences account for the residence to bending deformation in the SMA materials, and also for the bending rigidity which allows the brain incision to be held open in a particular shape during the operation. In the next section, the bending deformation properties of brain spatulas made of these materials will be discussed.

4. Bending characteristics of copper and SMA brain spatulas

In order to design an SMA brain spatula, it is important to evaluate the force required for bending of the spatula in operational use and the bending rigidity required for brain incision to be held open during the operation. With a focus on these two bending deformation properties in spatulas made of copper and SMA, the required specifications for an SMA brain spatula will be clarified. Conceiving of the existing type of brain spatula as a bendable cantilever made of a strip of material with a uniform rectangular cross-section, the length of the strip can be expressed by l, the width of the cross-section by w and the thickness by t.

Table 1. Values of modulus of elasticity, yield stress, yield strain and hardening modulus for copper, rolled SMA and cast SMAs

Materials	Copper	Rolled SMA (M-phase)	Cast SMA (M-phase)
Modulus of elasticity E [GPa]	95	40	54
Yield stress σ_M [MPa]	240	68	168
Yield strain ε_M [%]	0.25	0.17	0.34
Hardening modulus k [GPa]	0	2.6	2.5

4.1. Bending rigidity required to hold the brain spatula in its bent form

In order to maintain the chosen displacement in the part of the brain that is opened during the operation, it is required that the brain spatula should remain stable in its bent form (see Fig. 1). This requirement can be quantified in terms of the maximum permitted deflection in a cantilever made of the specified materials. Let us consider, in particular, the conditions required in each case for obtaining the same maximum deflection y_{max} in response to the same force F applied at the top of the cantilever. The maximum deflection of the cantilever y_{max} can be expressed using the second moment of area $I_z = wt^3/12$ from the theory of elasticity as follows

$$y_{max} = \frac{Fl^3}{3EI_z} = \frac{4Fl^3}{Ewt^3} \tag{4.1}$$

Assuming that this maximum deflection y_{max} in strips subjected to the same force F coincides for the copper and SMA materials, the following equation is obtained

$$y_{max} = \frac{4Fl_{Cu}^3}{E_{Cu}w_{Cu}t_{Cu}^3} = \frac{4Fl_{SMA}^3}{E_{SMA}w_{SMA}t_{SMA}^3} \tag{4.2}$$

From the practical point of view of a brain operation, the width w and the length l of an SMA brain spatula are expected to offer the same values as for a conventional spatula made of copper. Therefore, it is appropriate to assume that the length and width dimensions of both kinds of spatula will coincide, leaving only the thickness t to differ. The thickness for the SMA spatula t_{SMA} can be found from Eq. (4.2) as follows

$$t_{SMA} = t_{Cu}\sqrt[3]{\frac{E_{Cu}}{E_{SMA}}} \tag{4.3}$$

If the values for the modulus of elasticity shown for the copper and SMA materials in Table 1 are now substituted in Eq. (4.3), the bending rigidities of the three types of spatulas will be found to coincide when the rolled SMA spatula has a thickness of 1.3 times, and the cast SMA spatula a thickness of 1.2 times that of the copper spatula. These are the conditions, in other words, in which the same deflection and bending rigidity can be obtained from the SMA brain spatulas as from the copper one.

4.2. Force required to bend brain spatula

In a brain operation, the surgeon has to bend the spatula to fit the exact shape and depth of the part of the brain being opened. The force required to bend the brain spatula is evaluated as

the force applied at the top of the cantilever to obtain the required maximum bending strain. As shown in Fig. 6a, the yield (transformed) regions of the strip during bending occur at the inner and outer surfaces of the cantilever. A schematic stress-strain diagram and the distributions of bending strains and stresses in the strip are shown in Figs. 6b, and 7, respectively. In Fig. 6b, it is assumed that the yielding region can be expressed by the linear hardening with a hardening modulus k while the yield stress and yield strain are expressed by σ_M and ε_M, respectively. In these figures, the maximum bending stress and strain are denoted by σ_m and ε_m, respectively. It is assumed that the yield stress σ_M is the same in tension as in compression.
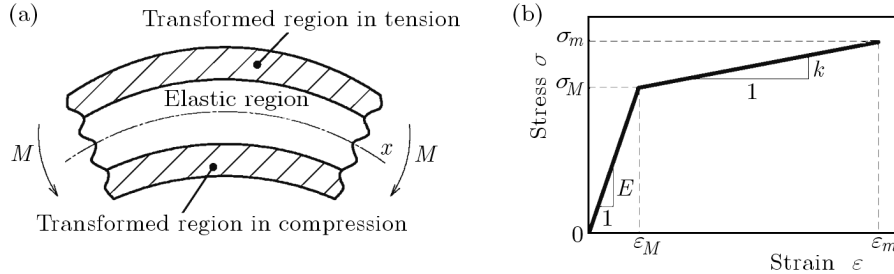

Fig. 6. (a) Elastic and transformed regions of the specimen in bending; (b) stress-strain diagram
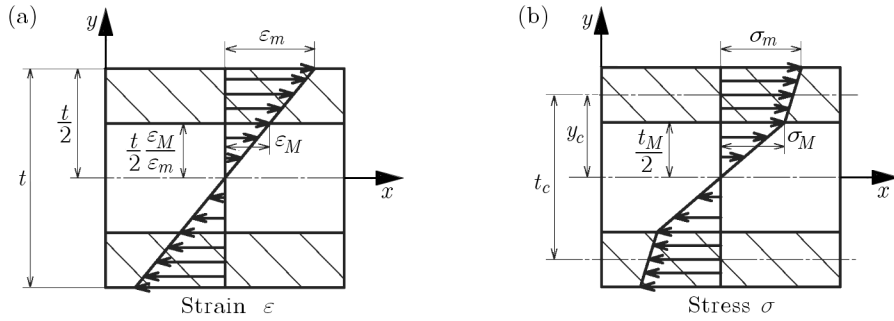

Fig. 7. Bending strain (a) and stress (b) distribution in the specimen

Let us first consider the bending moment M_e required to produce the elastic region of the strip in bending. The thickness of the elastic region t_M is $t_M = (\varepsilon_M/\varepsilon_m)t$. Since the maximum bending stress in the elastic region σ_{max} is the same as the yield stress σ_M, the bending moment required for the elastic region M_e is $M_e = \sigma_M Z$, where Z denotes the section modulus and $Z = wt_M^2/6$. Accordingly, the bending moment M_e for the elastic region is

$$M_e = \frac{\sigma_M w t^2}{6}\left(\frac{\varepsilon_M}{\varepsilon_m}\right)^2 \tag{4.4}$$

Next, let us turn our attention to the bending moment M_y required to create the yield (transformed) region of the strip. The center of the yield region y_c from the neutral axis z is calculated as

$$y_c = \frac{t_c}{2} = \frac{t}{4}\left(1 + \frac{\varepsilon_M}{\varepsilon_m}\right) \tag{4.5}$$

The area A_y of the yield region in the tension side of the cross section is

$$A_y = \frac{wt}{2}\left(1 - \frac{\varepsilon_M}{\varepsilon_m}\right) \tag{4.6}$$

Considering the stress distribution in the yield region and the symmetric match between the tension and compression sides, the bending moment M_y required to create the yield region is obtained as follows

$$M_y = \frac{1}{2}(\sigma_M + \sigma_m)A_y t_c = \frac{1}{8}[2\sigma_M + k(\varepsilon_m - \varepsilon_M)]wt^2\Big[1 - \Big(\frac{\varepsilon_M}{\varepsilon_m}\Big)^2\Big] \tag{4.7}$$

The total bending moment M required to bend the brain spatula is the sum of the bending moment M_e for the elastic region and the bending moment M_y for the yield region

$$M = M_e + M_y = \frac{wt^2}{24}\Big\{2\sigma_M\Big[3 - \Big(\frac{\varepsilon_M}{\varepsilon_m}\Big)^2\Big] + 3k(\varepsilon_m - \varepsilon_M)\Big[1 - \Big(\frac{\varepsilon_M}{\varepsilon_m}\Big)^2\Big]\Big\} \tag{4.8}$$

Since the bending moment $M = Fl$, the force required is

$$F = \frac{wt^2}{24l}\Big\{2\sigma_M\Big[3 - \Big(\frac{\varepsilon_M}{\varepsilon_m}\Big)^2\Big] + 3k(\varepsilon_m - \varepsilon_M)\Big[1 - \Big(\frac{\varepsilon_M}{\varepsilon_m}\Big)^2\Big]\Big\} \tag{4.9}$$

The condition that the forces required to bend a copper spatula with $k = 0$ and an SMA spatula coincide can be expressed as follows

$$\begin{aligned}
F &= \frac{\sigma_{MCu} w_{Cu} t_{Cu}^2}{12 l_{Cu}}\Big[3 - \Big(\frac{\varepsilon_{MCu}}{\varepsilon_{mCu}}\Big)^2\Big] \\
&= \frac{w_{SMA} t_{SMA}^2}{24 l_{SMA}}\Big\{2\sigma_{MSMA}\Big[3 - \Big(\frac{\varepsilon_{MSMA}}{\varepsilon_{mSMA}}\Big)^2\Big] + 3k_{SMA}(\varepsilon_{mSMA} - \varepsilon_{MSMA})\Big[1 - \Big(\frac{\varepsilon_{MSMA}}{\varepsilon_{mSMA}}\Big)^2\Big]\Big\}
\end{aligned} \tag{4.10}$$

If the length l, the width w and the maximum bending strain ε_m of both spatulas coincide only the thickness to differ, the thickness of the SMA brain spatula is

$$t_{SMA} = t_{Cu}\sqrt{\frac{2\sigma_{MCu}\Big[3 - \Big(\frac{\varepsilon_{MCu}}{\varepsilon_m}\Big)^2\Big]}{2\sigma_{MSMA}\Big[3 - \Big(\frac{\varepsilon_{MSMA}}{\varepsilon m}\Big)^2\Big] + 3k_{SMA}(\varepsilon_m - \varepsilon_{MSMA})\Big[1 - \Big(\frac{\varepsilon_{MSMA}}{\varepsilon m}\Big)^2\Big]}} \tag{4.11}$$

The yield stress σ_M, the yield strain ε_M and the hardening modulus k for the three types of materials are shown in Table 1. Using these values, the thickness of the SMA brain spatula t_{SMA} can be obtained from Eq. (4.11). The calculated relations between the thickness ratio t_{SMA}/t_{Cu} and the maximum bending strain ε_m are shown in Fig. 8. If the material of the thickness t_{SMA}
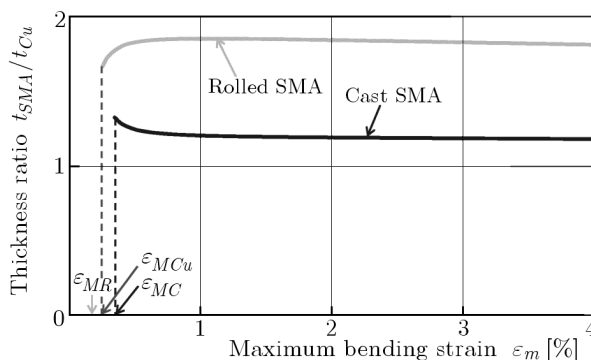

Fig. 8. Relationship between the thickness ratio t_{SMA}/t_{Cu} and the maximum bending strain ε_m calculated from Eq. (4.11)

shown in this figure is used, an SMA spatula can be bent by the same force as that required for a conventional copper spatula. As can also be seen from Fig. 8, the maximum bending strain ε_m exerts very little effect on the ratio of t_{SMA} to t_{Cu} except in an area of small ε_m values close to the yield strain ε_M. When the thicknesses of the rolled and cast SMA spatulas are 1.85 times and 1.20 times that of the copper spatula, respectively, the SMA spatula can be bent by applying the same force as with an existing copper spatula.

4.3. Shape of SMA brain spatula

The discussion in Sections 4.1 and 4.2 will have made clear that if the length and the width of a rolled SMA brain spatula are the same as those of the existing copper type while the thickness is 1.3 times as large, the rolled SMA spatula is capable of the same bending rigidity and can be easily bent using a smaller force than required for the copper one. Similarly, if the thickness of the cast SMA spatula is 1.2 times that of the copper one, the cast SMA spatula is capable of the same bending rigidity and can be bent by the same force as an existing copper one.

5. Bending fatigue properties

5.1. Fatigue life in alternating-plane bending

Figure 9 shows the relationship between the maximum bending strain ε_m and the number of cycles to failure N_f for the rolled SMA, the cast SMA and the copper one, as obtained from the alternating-plane bending fatigue test. For all three materials, the larger the ε_m, the smaller the N_f. It can also be seen that the fatigue life of the rolled SMA is 100 times longer than that of the copper, and that the fatigue life of the cast SMA is also 100 times longer that of the copper in the region where ε_m is small and 10 times longer in the region where it is large. The fatigue life of the copper is several hundred cycles at $\varepsilon_m = 1\%$, which is almost the same as the low-cycle fatigue life of normal metals (Shigley and Mischke, 1989). In the case of copper, the yield strain is caused by slip in the crystals and plastic deformation occurs repeatedly, resulting in short fatigue life. In the SMAs, the yield strain is not caused by permanent slip but by a recoverable rearrangement of the M-phase, which accounts for the long fatigue life. In the case of the cast SMA, as already observed in Fig. 4, stress increases with an increase in strain, and this in turn results in the shortening of the fatigue life with an increase in the maximum bending strain. The influence of the frequency on the fatigue life of the three materials is not clear for $f = 3.33\,\mathrm{Hz}$ and $8.33\,\mathrm{Hz}$. For the case of a TiNi SMA wire, it has been found that the lower the frequency, the longer the fatigue life (Tobushi *et al.*, 2000). This being so, the frequency of an SMA brain spatula in practical use should be lower than this range between $3.33\,\mathrm{Hz}$ and $8.33\,\mathrm{Hz}$. In practice, therefore, the actual fatigue life of the material in use will be longer than that obtained in the present study.
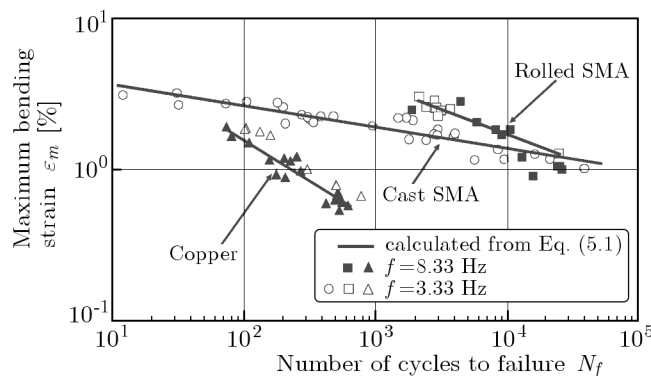

Fig. 9. Fatigue life curves for copper, rolled SMA and cast SMA under alternating-plane bending

In the low-cycle fatigue region of Fig. 9, the fatigue life curves of all three materials tested can be approximated by straight lines. Since the relationship between ε_m and N_f can also be expressed by a straight line on the logarithmic graph, the relationship can be expressed by a

power function similar to the fatigue life for TiNi SMA wires and tubes (Matsui *et al.*, 2004) as follows

$$\varepsilon_m N_f^{\beta} = \alpha \tag{5.1}$$

where α denotes ε_m at $N_f = 1$ and β denotes the slope of the $\log \varepsilon_m - \log N_f$ curve, respectively. The results calculated from Eq. (5.1) with values of $\beta = 0.58$ and $\alpha = 0.25$ for copper, $\beta = 0.41$ and $\alpha = 0.67$ for the rolled SMA and $\beta = 0.14$ and $\alpha = 0.05$ for the cast SMA are shown by solid lines in Fig. 9. As can be seen, these calculated results generally match up well with the inclinations obtained by testing.

5.2. Fatigue life in pulsating-plane bending

Figure 10 shows the relationship between maximum bending strain ε_m and the number of cycles to failure N_f for the rolled SMA, the cast SMA and the copper one, as obtained from the pulsating-plane bending fatigue test. Here too, the larger the ε_m, the smaller the N_f for all three materials. The fatigue life of the rolled SMA is 100 times longer than that of the copper, and that of the cast SMA is 40 times longer. The fatigue life of the copper is two thousand cycles at $\varepsilon_m = 2\%$. Again as observed in Fig. 4, the yield stress is higher for the cast SMA than for the rolled SMA, resulting in shorter fatigue life.
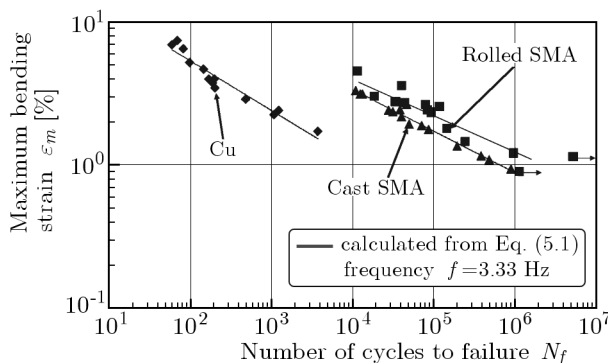

Fig. 10. Fatigue-life curves for copper, rolled SMA and cast SMA used for brain spatula under pulsating-plane bending

As in Fig. 9, the fatigue life curves of all three materials in the low-cycle fatigue region can be approximated by straight lines, meaning that the relationship can be expressed by a power function of Eq. (5.1). The calculated results from Eq. (5.1) with $\beta = 0.35$ and $\alpha = 0.26$ for copper, $\beta = 0.26$ and $\alpha = 0.43$ for the rolled SMA and $\beta = 0.29$ and $\alpha = 0.49$ for the cast SMA are shown by the solid lines in Fig. 10. As can be seen, these calculated results again show a good overall match with the test inclinations.

5.3. Comparison of fatigue life

The relationships between the maximum bending strain ε_m and the number of cycles to failure N_f obtained from the alternating- and pulsating-plane bending fatigue tests are brought together in Fig. 11 for the rolled, and in Fig. 12 for the cast SMA. In both cases, the fatigue life is shorter in alternating-plane bending than in pulsating-plane bending. Since the amount of work dissipated in each cycle is greater in the case of alternating-plane bending, a longer fatigue life can be obtained for an SMA brain spatula in use by fixing the bending direction to result in pulsating bending. The influence of the dissipated work W_d on the difference in fatigue life between the cases of alternating- and pulsating-plane bending can be explained as follows. The stress-strain relations and the amount of work dissipated W_d at each cycle of pulsating-

or alternating-plane bending are shown, respectively, in diagrams (a) and (b) in Fig. 13, where it is assumed that the yielding region is expressed by the linear hardening with a hardening modulus k and that the yield stress σ_M is constant under cyclic deformation and has the same value under tension and compression. The area enclosed by the hysteresis loop gives a measure of the work dissipated W_d per unit volume in each cycle.
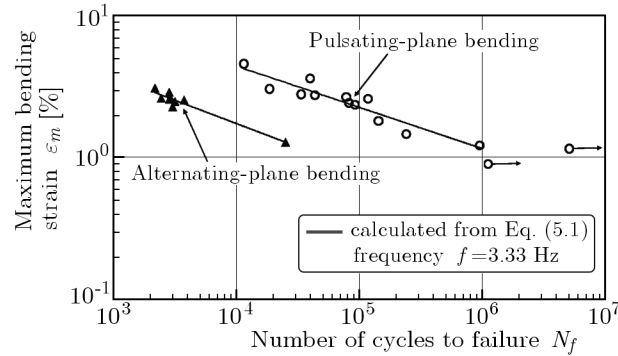
Fig. 11. Relationship between the maximum bending strain and number of cycles to failure for the rolled SMA under alternating-plane and pulsating-plane bending
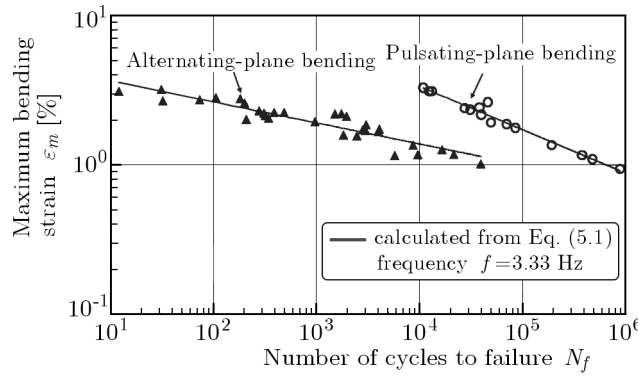
Fig. 12. Relationship between the maximum bending strain and number of cycles to failure for the cast SMA under alternating-plane and pulsating-plane bending
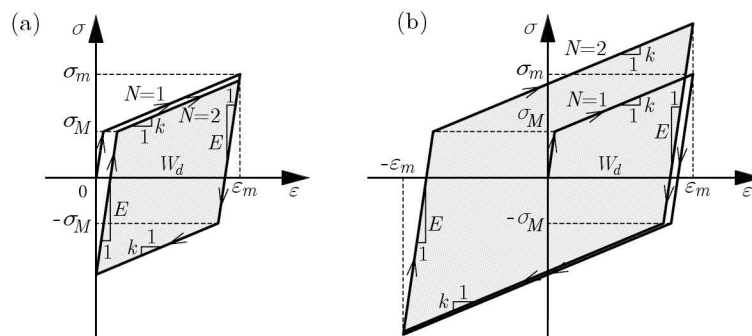
Fig. 13. Stress-strain diagram and dissipated work W_d in the initial cycle under pulsating-plane bending (a) and alternating-plane bending (b)

The work dissipated in $N = 2$ is expressed by the following equation for the pulsating-plane bending

$$W_d = \left(1 - \frac{k}{E}\right)\left[\sigma_M\left(2 - \frac{k}{E}\right) + k\left(1 - \frac{k}{E}\right)\left(\varepsilon_m - \frac{\sigma_M}{E}\right)\right]\left[\left(1 - \frac{k}{E}\right)\left(\varepsilon_m - \frac{\sigma_M}{E}\right) - \frac{\sigma_M}{E}\right] \quad (5.2)$$

while the work dissipated for the same cycle of alternating-plane bending is

$$W_d = 4\frac{E-k}{E+k}\Big(\varepsilon_m - \frac{\sigma_M + k\varepsilon_m}{E+k}\Big)(\sigma_M + k\varepsilon_m) \tag{5.3}$$

where E and ε_m represent the elastic modulus and the maximum bending strain in each cycle, respectively. It can be seen from Eqs. (5.2) and (5.3) that W_d increases in proportion to both σ_M and ε_m. The quantitative relationship between the fatigue life N_f and dissipated work W_d obtained from Eqs. (5.2) and (5.3) is shown in Fig. 14 for the rolled, and in Fig. 15 for the cast SMA. In both cases, the relationship between N_f and W_d can be matched approximately by a single straight line taking in both the alternating- and the pulsating-plane bending. In other words, the unified relationship between the fatigue life N_f and dissipated work W_d under both alternating- and pulsating-plane bending can be expressed by the same power function

$$W_d N_f^\lambda = \mu \tag{5.4}$$

where μ and λ denote W_d in $N_f = 1$ and the slope of the $\log W_d - \log N_f$ curves, respectively. Results calculated from this equation are shown by the solid lines in Fig. 14, with values of $\lambda = 0.45$ and $\mu = 408\,\mathrm{MJ/m^3}$, for the rolled SMA and in Fig. 15, with values of $\lambda = 0.29$ and $\mu = 88\,\mathrm{MJ/m^3}$, for the cast SMA. As can be seen, the solid lines show a good overall match with the test results. In the case of the rolled SMA in Fig. 14, the range $2 \cdot 10^3 \leqslant N_f \leqslant 5 \cdot 10^4$, in the number of cycles to failure represents the fatigue life under alternating-plane bending, while the range $2 \cdot 10^4 \leqslant N_f \leqslant 1 \cdot 10^6$ represents that under pulsating-plane bending. The corresponding ranges for the cast SMA in Fig. 15 are $1 \cdot 10^1 \leqslant N_f \leqslant 3 \cdot 10^4$ cycles under alternating-plane bending and $1 \cdot 10^4 \leqslant N_f \leqslant 1 \cdot 10^6$ cycles under pulsating-plane bending. For the cast SMA, the value of W_d is much larger under alternating-plane bending than under pulsating-plane bending. That is why the fatigue life of a cast SMA is shorter under alternating-plane bending for a large maximum bending strain ε_m. To sum up, as already mentioned above, the unified relationship between W_d and N_f is of great usefulness for evaluating the fatigue life of a rolled SMA or a cast SMA under conditions of either alternating- or pulsating-plane bending.
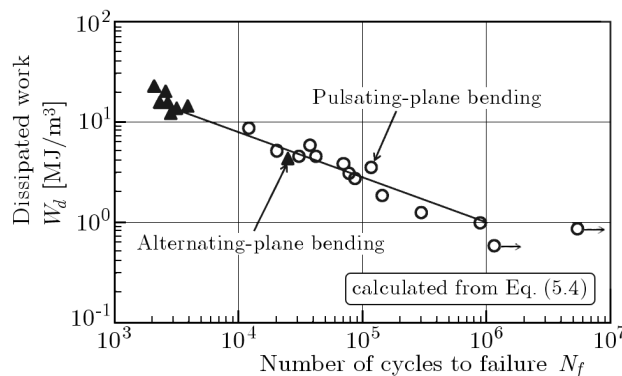

Fig. 14. Relationship between the dissipated work W_d and number of cycles to failure for the rolled SMA under alternating-plane and pulsating-plane bending

5.4. Temperature rise under cyclic bending

The surface portion of the specimen is subjected to the effects of dissipated work in each cycle as discussed in Section 5.3. Therefore, the temperature of the specimen can be expected to increase under cyclic bending. The surface temperature in the central part of a rolled SMA strip was measured using a thermocouple under conditions of alternating-plane bending at a frequency of $f = 3.33\,\mathrm{Hz}$. The relationship between the incremental temperature rise ΔT and
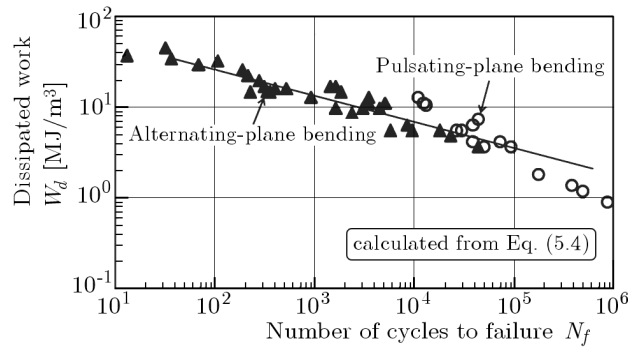
Fig. 15. Relationship between the dissipated work W_d and number of cycles to failure for the cast SMA under alternating-plane and pulsating-plane bending
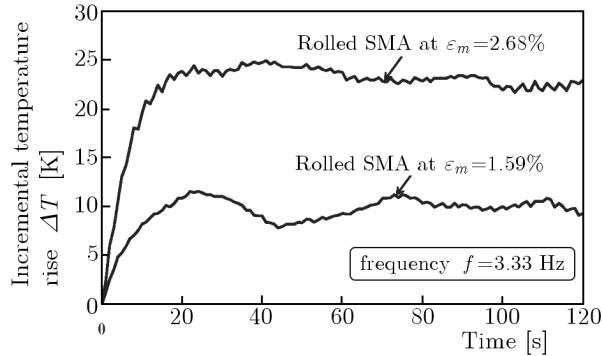
Fig. 16. Relationships between the incremental temperature rise and time for the rolled SMA at two different maximum bending strains, under alternating-plane bending at $f = 3.33\,\mathrm{Hz}$
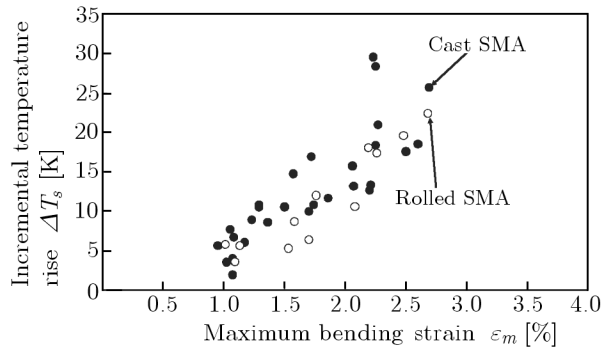
Fig. 17. Relationships between the temperature rise saturation points and maximum bending strains, for the rolled and cast SMAs under alternating-plane bending at at $f = 3.33\,\mathrm{Hz}$

time is shown in Fig. 16. In the first 20 seconds or so, the temperature increases rapidly, but once the amount of heat generated comes to match the amount released a saturation level is reached for ΔT.

The relationship between the saturation point for the temperature rise ΔT_s and the maximum bending strain ε_m is shown in Fig. 17 for the rolled and the cast SMAs at $f = 3.33\,\mathrm{Hz}$. The saturation point increases in proportion to the rise in ε_m. The value of ΔT_s is a little higher for the cast than for the rolled SMA, rising to around $30\,\mathrm{K}$ at $\varepsilon_m = 3\%$. The yield stress σ_M also increases with temperature, at a rate of $5\,\mathrm{MPa/K}$ in the case of a TiNi SMA. For $\Delta T = 30\,\mathrm{K}$, this gives a yield stress increase of $150\,\mathrm{MPa}$. This explains why the fatigue damage is large under alternating-plane bending for a large ε_m. In practical use in a brain spatula, the frequency will be low and the temperature rise only small, resulting in a much longer fatigue life than that obtained in the present study.

6. Conclusions

In order to develop the SMA-brain spatula, the mechanical characteristics of the TiNi cast- and rolled-SMAs and the copper one used for the brain spatula were compared based on the tensile deformation properties, and the characteristics of the SMA-brain spatula were discussed. The fatigue properties of these materials were also investigated by pulsating- and alternating-plane bending fatigue tests. The results obtained can be summarized as follows.

(1) Based on the yield stress and the modulus of elasticity of the copper and the TiNi SMAs, the bending deformation properties of the SMA-brain spatula were estimated by assuming the condition to use the brain spatula as the bending of the strip cantilever. With respect to the SMA-brain spatula for the same length and width as the existing copper one, if the thickness of the conventional rolled-SMA spatula is 1.3 times as large as that of the existing copper-brain spatula, the SMA spatula can hold the same bending rigidity and can be bent by a smaller force than the existing copper one. If the thickness of the new cast-SMA spatula is 1.2 times as large as that of the existing-copper spatula, the SMA spatula can hold the same bending rigidity and can be bent by the same force as the existing copper one.

(2) With respect to the alternating- and pulsating-plane bending fatigue, the fatigue life of both the copper and the SMAs in the region of low-cycle fatigue is expressed by a power function of the maximum bending strain. The fatigue life of the conventional rolled SMA and the new cast SMA is longer than that of the existing copper. The fatigue life of the rolled SMA is longer than that of the cast SMA. The fatigue life of the new cast and rolled SMAs in the pulsating-plane bending is longer than that in the alternating-plane bending. The fatigue life of the rolled SMA and cast SMA for alternating- and pulsating-plane bendings can be expressed by the unified relationship with a power function of the dissipated work.

(3) The above mentioned characteristics of the SMA-brain spatula obtained in this study will be substantially applied to the development not only for the brain spatula but also for other retractors and instruments used in other surgery operations.

References

1. CHU Y.Y., ZHAO L.C., EDS., 2002, *Shape Memory Materials and Its Applications*, Trans. Tech. Pub., Switzerland

2. DUERIG T.W., MELTON K.N., STOCKEL D., WAYMAN C.M., EDS., 1990, *Engineering Aspects of Shape Memory Alloys*, Butterworth-Heinemann, 1-35

3. FUNAKUBO H., ED., 1987, *Shape Memory Alloys*, Gordon and Breach Science Pub., 1-60

4. FURUICHI Y., TOBUSHI H., IKAWA T., MATSUI R., 2003, Fatigue properties of a TiNi shape-memory alloy wire subjected to bending with various strain ratios, *Proc. Instn. Mech. Engrs.*, **217**, *Part L: Materials: Design and Applications*, 93-99

5. MATSUI R., TOBUSHI H., FURUICHI Y., HORIKAWA H., 2004, Tensile deformation and rotating-bending fatigue properties of a highelastic thin wire, a superelastic thin wire, and a superelastic thin tube of NiTi alloys, *Trans. ASME, J. Eng. Mater. Tech.*, **126**, 384-391

6. OTSUKA K., WAYMAN C.M., EDS., 1998, *Shape Memory Materials*, Cambridge University Press, Cambridge

7. SABURI T., ED., 2000, *Shape Memory Materials*, Trans. Tech. Pub., Switzerland

8. SHIGLEY J.E., MISCHKE C.R., 1989, *Mechanical Engineering Design*, 5th ed., McGraw-Hill, New York, 270-274

9. TOBUSHI H., NAKAHARA T., SHIMENO Y., HASHIMOTO T., 2000, Low-cycle fatigue of TiNi shape memory alloy and formulation of fatigue life, *Trans. ASME, J. Eng. Mater. Tech.*, **122**, 186-191

10. TOBUSHI H., OKUMURA K., NAKAGAWA K., TAKATA K., 2001, Fatigue properties of TiNi shape memory alloy, *Trans. Mater. Res. Soc. Jap.*, **26**, 1, 347-350

11. TOBUSHI H., TANAKA K., KIMURA K., HORI T., SAWADA T., 1992, Stress-strain-temperature relationship associated with the R-phase transformation in TiNi shape memory alloy, *JSME Inter. J., Ser. I*, **35**, 3, 278-284

12. YOSHIMI Y., KITAMURA K., TOKUDA M., INABA T., ASAI J., WATANABE Y., 2008, Ti-Ni shape memory alloys precision casting products and its process, *Proc. Int. Conf. Shape Memory and Superelastic Tech.*, 387-396

Konstrukcja i właściwości użytkowe odlewanej szpatułki chirurgicznej wykonanej ze stopu z pamięcią kształtu

Streszczenie

W pracy opisano problem projektowania szpatułki używanej w chirurgii mózgu, wykonanej ze stopu z pamięcią kształtu (SMA). Przedyskutowano charakterystyki zginania nowej szpatułki wykonanej z precyzyjnie odlewanego stopu TiNi. Wyniki badań podsumowano w następujący sposób: (1) w porównaniu do konwencjonalnych, miedzianych szpatułek o tej samej długości i szerokości, jeśli odlewana szpatułka SMA jest 1.2 raza grubsza od miedzianej, lub 1.3 raza, gdy wykonana została przez walcowanie, instrument ten będzie posiadał taką samą sztywność giętną i wytrzyma niemalże to samo obciążenie zginające, jak w przypadku narzędzia miedzianego; (2) wyrażając wytrzymałość zmęczeniową szpatułki miedzianej w rejonie niskocyklicznych obciążeń jako funkcję potęgową maksymalnego odkształcenia przy zginaniu, stwierdzono, że szpatułki SMA wykazują dłuższą żywotność od konwencjonalnych. W obydwu przypadkach – odlewanej i walcowanej szpatułki SMA – wytrzymałość zmęczeniowa jest większa dla płaskiego jednostronnego zginania od wytrzymałości przy zginaniu przemiennym.